molecular pharmaceutics

Article

pubs.acs.org/molecularpharmaceutics

Design and Biological Evaluation of Cell-Penetrating Peptide–Doxorubicin Conjugates as Prodrugs

Amir Nasrolahi Shirazi, Rakesh Tiwari, Bhupender S. Chhikara, Dindyal Mandal, and Keykavous Parang*

Department of Biomedical and Pharmaceutical Sciences, College of Pharmacy, University of Rhode Island, 7 Greenhouse Road, Kingston, Rhode Island 02881, United States

Supporting Information

ABSTRACT: Doxorubicin (Dox) is a hydrophilic anticancer drug that has short retention time due to the efficient efflux in some cancer cells (e.g., ovarian adenocarcinoma SK-OV-3). Cyclic [W(RW)$_4$] and the corresponding linear peptide (RW)$_4$ were conjugated with Dox through an appropriate linker to afford cyclic [W(RW)$_4$]–Dox and linear (RW)$_4$–Dox conjugates to enhance the cellular uptake and cellular retention of the parent drug for sustained anticancer activity. Comparative antiproliferative assays between covalent (cyclic [W(RW)$_4$]–Dox and linear (RW)$_4$–Dox) and the corresponding noncovalent physical mixtures of the peptides and Dox were performed. Cyclic [W(RW)$_4$]–Dox inhibited the cell proliferation of human leukemia (CCRF-CEM) (62–73%), ovarian adenocarcinoma (SK-OV-3) (51–74%), colorectal carcinoma (HCT-116) (50–67%), and breast carcinoma (MDA-MB-468) (60–79%) cells at a concentration of 1 μM after 72–120 h of incubation. Cyclic [W(RW)$_4$]–Dox exhibited higher antiproliferative activity than linear (RW)$_4$–Dox in all cancer cells with the highest activity observed after 72 h. Flow cytometry analysis showed 3.6-fold higher cellular uptake of cyclic [W(RW)$_4$]–Dox than Dox alone in SK-OV-3 cells after 24 h incubation. The cellular hydrolysis study showed that 99% of cyclic [W(RW)$_4$]–Dox was hydrolyzed intracellularly within 72 h and released Dox. These data suggest that cyclic [W(RW)$_4$]–Dox can be used as a potential prodrug for improving the cellular delivery and retention of Dox.

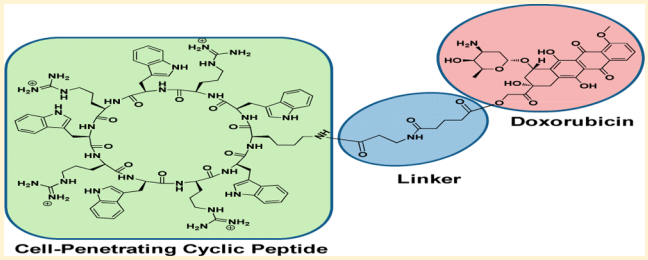

KEYWORDS: *anticancer, cellular uptake, doxorubicin, cyclic peptides, cell-penetrating peptides*

INTRODUCTION

Doxorubicin (Dox) is a well-known anthracycline and widely used anticancer agent for the treatment of a wide variety of cancers, such as breast carcinoma, leukemia, and other solid tumors.[1] The major mechanism of Dox activity is the inhibition of topoisomerase II (TOPO II)–DNA complex, causing DNA damage through intercalating with the DNA double helix.[2]

One of the major limitations of cancer chemotherapy treatment is the development of resistance to a certain dose of anticancer drugs, such as Dox. Several mechanisms of drug resistance have been introduced at different levels, including alteration of the target protein, decreased membrane permeability and drug metabolism, and/or efflux pumping.[3−5] Dox is not being used widely for treating other tumors like ovarian carcinoma, liver cancer, and stomach cancer in the clinic,[6,7] due to the development of resistance associated with Dox. Furthermore, the use of Dox for clinical application revealed undesired pharmacokinetics properties, such as rapid distribution, excretion, and low bioavailability of the drug, due to the hydrophilic nature, high volume of distribution, and short half-life.[8−10] Thus, a high cumulative dose of Dox is required in cancer chemotherapy to achieve a sufficient therapeutic effect, which leads to dose-dependent side effects, such as such as cumulative cardiotoxicity, nephrotoxicity, and extravasation.[11,12]

Moreover, intracellular Dox accumulation is dependent on a number of factors including cellular uptake, retention, relocalization, and efflux from the cell. Among these factors, intracellular uptake of Dox suffers from efflux pumping in some cancer cells, such as ovarian carcinoma cells, leading to decreased intracellular Dox levels that could be related to the overexpression of energy-dependent drug efflux pump proteins such as P-glycoprotein (P-gp). This integral membrane protein removes drugs and thus reduces intracellular anticancer drug concentrations.[13]

Efficacy and toxicity of an anticancer drug can be modified through using drug delivery systems and altering the physicochemical properties, such as lipophilicity, cellular uptake, and prolonging activity through chemical conjugation with various chemical moieties. One of the main applications of drug delivery systems is to avoid the P-gp and multidrug resistance proteins (MRPs) that are involved in drug efflux to

Special Issue: Prodrug Design and Target Site Activation

Received: July 24, 2012
Revised: January 8, 2013
Accepted: January 9, 2013
Published: January 9, 2013

ACS Publications © 2013 American Chemical Society

Scheme 1. Synthesis of Linear $(RW)_4$ Peptide

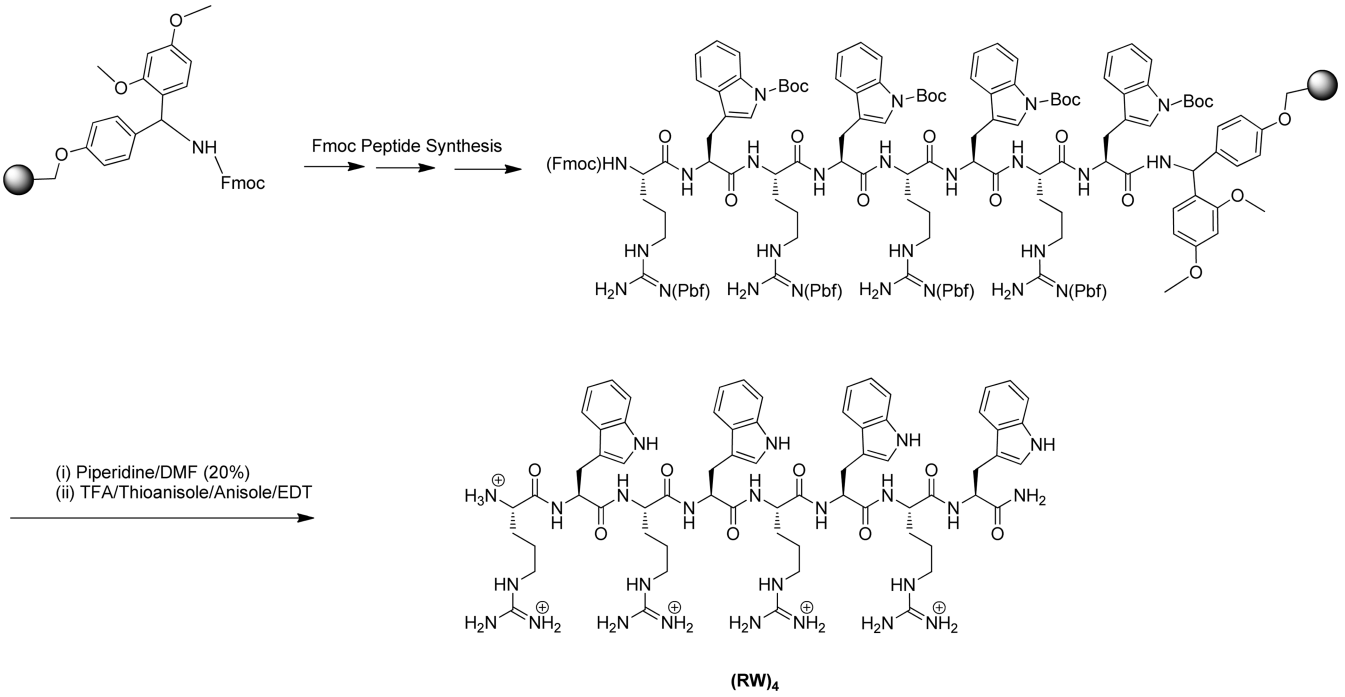

overcome the resistance problem and P-gp-mediated drug efflux.[14−16]

Prodrug strategy as one of the drug delivery systems through chemical conjugation with a parent drug[17,18] has been widely used in Dox delivery.[6,19] Several conjugation methods have been used to improve Dox delivery, including using gold nanoparticles,[20] gold nanospheres,[21] liposomes,[22] peptides,[23−27] and dendrimers.[28] Conjugation of Dox with cell-penetrating peptides (CPPs) has been employed as one of the privileged methods to translocate a wide variety of cargo molecules into various cell lines.[16] For instance, Dox has been conjugated with different linear CPPs including penetratin,[24] tat,[29] and polyarginine,[30] and maurocalcine.[31]

However, development of efficient and safe prodrug carriers to enhance delivery and retention of Dox into drug-resistant tumor cells and to reduce efflux remains less explored. We previously reported the application of a number of cyclic peptides as noncovalent nuclear targeting molecular transporters[32] of Dox. Cyclic peptides containing arginine and tryptophan $[WR]_n$ (n = 3−5) were found to be appropriate noncovalent carriers for Dox, however, the drug intracellular retention and toxicity behavior for cyclic peptide−Dox covalent conjugates remain unexplored. Herein, we report the synthesis of linear and cyclic peptides through the covalent conjugation with a 3-carbon chain linker at the 14-hydroxyl group, evaluation of their *in vitro* anticancer activities in multiple cancer cell lines, and cellular uptake and retention. The prodrug conjugates were designed to improve cellular uptake, to prolong biological activity, and to reduce intrinsic cellular efflux of Dox.

EXPERIMENTAL SECTION

Synthesis of Linear $(RW)_4$ Peptide. The linear peptide was assembled on Fmoc-Rink amide resin (0.56 g, 0.54 mmol/g, 0.3 mmol) by solid-phase peptide synthesis strategy using Fmoc-protected amino acids [Fmoc-Trp(Boc)-OH and Fmoc-Arg(Pbf)-OH] on a PS3 automated peptide synthesizer at room temperature (Scheme 1). Linear peptide sequence was assembled on the resin after removing the Fmoc group at the end of the sequence (NH_2-RWRWRWRW) $(RW)_4$, using 20% piperidine in DMF. The resin was washed with DCM (3 × 15 mL) and MeOH (3 × 15 mL) for complete cleavage of peptide from the resin and side chain protecting groups. The resin was dried in vacuum for 24 h. A cleavage cocktail, namely, reagent R containing TFA/thioanisole/EDT/anisole (90:5:3:2 v/v/v/v, 12 mL), was added to the resin. The mixture was shaken at room temperature for 2 h. The resin was collected by filtration and consequently washed with 2 mL of reagent R again. Collected filtrates were evaporated to reduce the volume under dry nitrogen. The crude peptide was precipitated by adding cold diethyl ether (200 mL, Et_2O) and centrifuged at 4000 rpm for 5 min followed by decantation to obtain the solid precipitate. The solid material was further washed with cold ether (2 × 100 mL) for 2 times. The peptide was lyophilized and purified by reversed-phase Hitachi HPLC using a gradient system as described in the Supporting Information to yield linear $(RW)_4$ peptide.

$(RW)_4$. MALDI-TOF (m/z) $[C_{68}H_{91}N_{25}O_8]$: calcd, 1385.7482; found, 1386.8219 $[M + H]^+$.

Synthesis of Cyclic Peptide [W(RW)$_4$K]β-Ala. The linear-protected peptides sequence was assembled using a PS3 automated peptide synthesizer. The linear protected peptide (Dde-K(Boc-β-Ala)(WRWRWRWRW) was assembled on the H-Trp(Boc)-2-chlorotrityl chloride resin (513 mg, 0.78 mmol/g, 0.40 mmol) in 0.40 mmol scale (Scheme 2). After the final coupling with Boc-β-Ala-OH, the resin was washed with DMF (3 × 25 mL, each time 5 min). Then the Dde group at the lysine N-terminal was deprotected by using hydrazine monohydrate (2% v/v) solution in DMF (3 × 25 mL, each time 5 min). The resin was washed with DMF (5 × 50 mL) followed by washing with DCM (3 × 50 mL). The side chain protected peptide was cleaved from trityl resin by using cleavage cocktail reagent, acetic acid/TFE/DCM (1:2:7 v/v/v,

dx.doi.org/10.1021/mp3004034 | Mol. Pharmaceutics 2013, 10, 488−499

Scheme 2. Synthesis of Cyclic [W(RW)$_4$K](β-Ala) Peptide

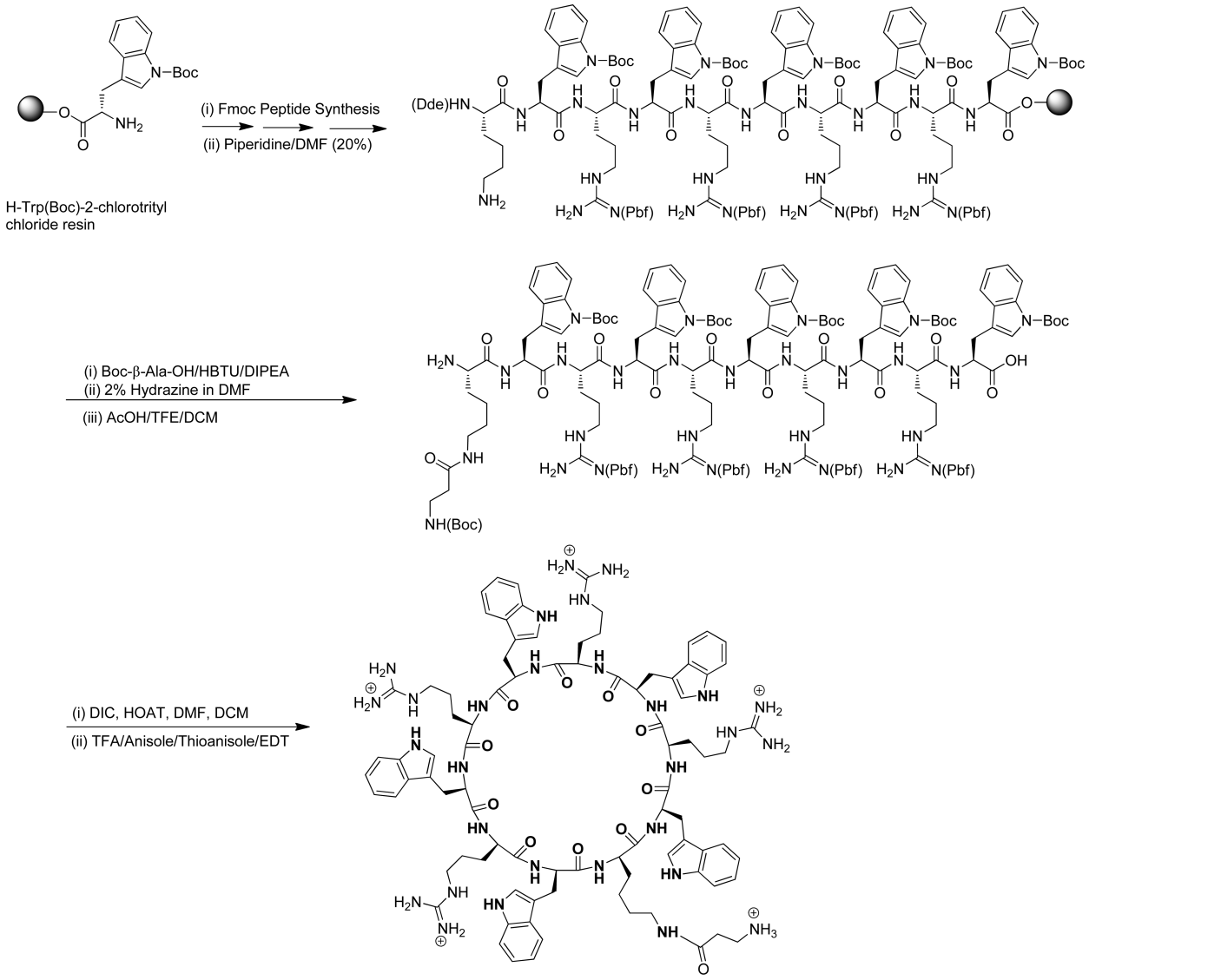

50 mL), by shaking for 1 h at room temperature to yield the side chain protected linear peptide. The resin was collected by filtration and washed with TFE/DCM (2:8 v/v, 2 × 10 mL). The combined filtrates were evaporated under reduced pressure. Hexane (2 × 25 mL) and DCM (1 × 25 mL) were added to the residue to remove the acetic acid from the cleaved crude peptide. The crude peptide was obtained as a white solid and was dried in vacuum overnight. The compound was directly used for the next cyclization reaction. The linear peptide was dissolved in DMF/DCM (5:1 v/v, 250 mL). 1-Hydroxy-7-azabenzotriazole (HOAt, 223 mg, 1.64 mmol, 4 equiv) and 1,3-diisopropylcarbodiimide (DIC, 290 μL, 1.86 mmol, 4.5 equiv) were added to the mixture, and the solution was stirred at room temperature for 6 h. The completion of the cyclization was checked by MALDI-TOF. After the reaction was completed, the solvents were removed under reduced pressure by using a rotary evaporator. The crude product was dried overnight in vacuum before the final cleavage reaction. The cleavage reaction was performed by using reagent R as previously described. The crude peptides were lyophilized and purified by reversed-phase Hitachi HPLC (L-2455) as described in the Supporting Information to yield cyclic peptide [W(RW)$_4$K(β-Ala)].

MALDI-TOF (m/z) [$C_{88}H_{115}N_{29}O_{11}$]: calcd, 1753.9331; found, 1756.6570 $[M + 3H]^+$.

Synthesis of *N*-Fmoc-Dox-14-*O*-hemiglutarate. The synthesis of this *N*-Fmoc Dox derivative was carried out according to the previously reported procedure.[33] In brief, Dox hydrochloride (100 mg, 0.17 mmol) was dissolved in anhydrous DMF (4 mL) in a round-bottom flask and stirred at room temperature under nitrogen atmosphere. Fmoc-OSu (60 mg, 0.18 mmol) was added to the reaction mixture followed by dropwise addition of anhydrous *N*,*N*-diisopropylethylamine (DIPEA, 60 μL, 0.34 mmol). Aluminum foil was used to cover the reaction vessel from light, and stirring of the reaction mixture was continued at room temperature. The reaction was stopped, and the solvent was removed after 4 h. The remaining oily liquid was triturated with 0.1% TFA solution in water (v/v) to afford crystalline solid compound. The crystalline solid was collected through filtration and washed with cold diethyl ether to remove traces of excess of Fmoc-OSu. HPLC analysis showed that the crude product was pure (95%). The Fmoc-*N*-Dox (110 mg, 0.14 mmol) was

dx.doi.org/10.1021/mp3004034 | *Mol. Pharmaceutics* 2013, 10, 488−499

Scheme 3. Synthesis of Dox−Peptide (Linear or Cyclic) Conjugates

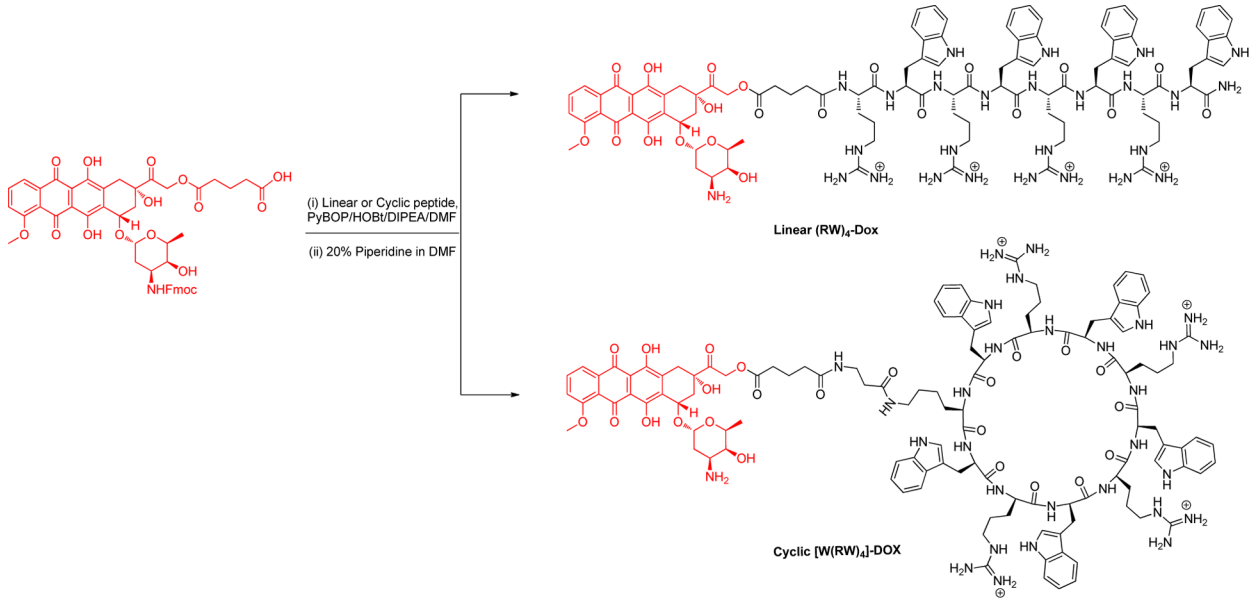

reacted with glutaric anhydride (19.7 mg, 0.17 mmol) in the presence of anhydrous DIPEA (46 μL, 0.26 mmol) in anhydrous DMF (5 mL) for 16 h under nitrogen atmosphere. Analytical HPLC analysis showed that the reaction was completed after 16 h. The solvent was removed under reduced pressure, and the oily liquid was triturated with 0.1% TFA solution in water (v/v) to precipitate the crude solid material. The crude solid material was filtered and dried in high vacuum. The material was purified by HPLC to afford pure *N*-Fmoc-Dox-14-*O*-hemiglutarate (95%).

General Procedure for Coupling of the Peptides to Dox. *N*-Fmoc-Dox-14-*O*-hemiglutarate (1 equiv), cyclic or linear peptide (1 equiv), benzotriazol-1-yloxytripyrrolidino-phosphonium hexafluorophosphate (PyBOP, 1.35 equiv), and hydroxybenzotriazole (HOBt, 2.70 equiv) were added to the glass vial under nitrogen atmosphere (Scheme 3). Anhydrous DMF (1−2 mL) was used as a solvent, and the reaction mixture was stirred to dissolve the compounds followed by the addition of DIPEA (8 equiv). Then, the reaction mixture was stirred for 1.5 h in the absence of light. The solvent was removed under reduced pressure, and cold diethyl ether was added to the residue. The crude peptide was precipitated and centrifuged to obtain the crude solid peptide conjugate. The peptide was dried under nitrogen gas. To remove the Fmoc group, a solution of piperidine in DMF was used (20% v/v, 2 mL for 5 min). The solution color turned to blue, and the reaction was terminated by adding drops of TFA solution in DMF (20% v/v) until the solution color turned to light red. The solvent was removed under reduced pressure, and oily liquid was dissolved in acetonitrile/water (50% v/v). The HPLC purification afforded the final linear peptide or cyclic peptide−Dox conjugates.

Cyclic [W(RW)$_4$]−Dox Peptide. ^{1}H NMR (DMSO-d_6, 500 MHz, δ ppm): 0.80−0.97 (m, 8H, $CH_2CH_2CH_2NH$, Arg), 1.10−1.25 (m, 13H, $CH_2CH_2CH_2NH$, Arg, Lys, 6′-CH_3), 1.89−2.25 (m, 4H, H-8 and H-2′), 2.40−2.67 (m, 14H, CH_2CO and $CH_2CH_2CH_2NH$), 2.90−3.20 (m, 12H, CH_2, Trp, H-10), 3.55−3.52 (m, H-3′, H-4′ overlapped with DMSO peaks), 3.99 (s, 3H, OCH_3), 4.20−4.40 (m, 6H, αCH, Arg, Lys, H-5′), 4.85−4.98 (m, 5H, αCH, Trp), 5.10−5.48 (m, 3H, H-7, OCH_2CO), 5.61−5.65 (m, 1H, H-1′), 6.27 (br s, 12 H, NH), 6.85−7.70 (m, aromatic, 25 H, Trp, aromatic CH), 7.75−8.00 (m, 4H, aromatic CH), 10.74 (br s, 5H, NH, Trp), 13.27 (s, 2H, PhOH). MALDI-TOF (*m*/*z*) [$C_{120}H_{148}N_{30}O_{24}$]: calcd, 2393.1283; found, 2393.5332 [M]$^+$.

Linear (RW)$_4$−Dox. MALDI-TOF (*m*/*z*) [$C_{100}H_{124}N_{26}O_{21}$]: calcd, 2024.9434; found, 2024.6139 [M]$^+$.

Cell Culture. Human leukemia carcinoma cell line CCRF-CEM (ATCC no. CCL-119), breast adenocarcinoma MDA-MB-468 (ATCC no. HTB-132), ovarian adenocarcinoma SK-OV-3 (ATCC no. HTB-77), and colorectal carcinoma HCT-116 (ATCC no. CCL-247) were obtained from American Type Culture Collection. The cells were grown on 75 cm^2 cell culture flasks with RPMI-16 medium for leukemia and EMEM medium for other cell lines and supplemented with 10% fetal bovine serum (FBS) and 1% penicillin−streptomycin solution (10,000 units of penicillin and 10 mg of streptomycin in 0.9% NaCl) in a humidified atmosphere of 5% CO_2, 95% air at 37 °C.

Antiproliferation Assay. Antiproliferative activities of covalently synthesized cyclic [W(RW)$_4$]−Dox, linear (RW)$_4$−Dox derivatives, and noncovalent mixtures of cyclic [RW]$_4$ + Dox and linear (RW)$_4$ + Dox were evaluated in MDA-MB-468, CCRF-CEM, SK-OV-3, and HCT-116 cells, and the results were compared with that of Dox alone. The assay was carried out using CellTiter 96 AQueous One Solution Cell Proliferation Assay Kit (Promega, USA). As a representative example, SK-OV-3 cells were suspended in 5 × 10^3/mL (CCRF-CEM, 4 × 10^4/mL), and 100 μL of the cell suspension was placed in each well of the 96 well culture plates. The cells were incubated with Dox (1 μM), cyclic [W(RW)$_4$]−Dox (1 μM), linear (RW)$_4$−Dox (1 μM), cyclic [RW]$_4$ (1 μM) + Dox (1 μM), and linear (RW)$_4$ (1 μM) + Dox (1 μM) in 2% DMSO and tested in triplicate. For the physical mixtures, an appropriate volume of Dox stock solution was mixed with an appropriate volume of an aqueous solution of cyclic and linear peptides physically to obtain a final concentration of Dox (1 μM) and the peptide (1 μM). The mixture was vigorously mixed and vortexed until the solution became homogeneous/clear red color. Subsequently, the mixture was incubated for 30 min at 37 °C before addition to the cells. Incubation was carried out at 37 °C in an incubator supplied with 5% CO_2 for

dx.doi.org/10.1021/mp3004034 | *Mol. Pharmaceutics* 2013, 10, 488−499

24−120 h. At the end of the sample exposure period (24−120 h), 20 μL of CellTiter 96 aqueous solution was added. The plate was returned to the incubator for 1 h in a humidified atmosphere at 37 °C. The absorbance of the formazan product was measured at 490 nm using a microplate reader. The percentage of cell survival was calculated as [(OD value of cells treated with the test compound) − (OD value of culture medium)]/[(OD value of control cells) − (OD value of culture medium)] × 100%.

Cell Cytotoxicity Assay. The cytotoxicity of Dox and cyclic $[W(RW)_4]$−Dox against MDA-MB-468, HCT-116, CCRF-CEM, and SK-OV-3 was determined by MTS assay using CellTiter 96 AQueous One Solution Cell Proliferation Assay Kit (Promega, USA). All cells were plated overnight in 96 well plates with a density of 5000 cells per well in 0.1 mL of appropriate growth medium at 37 °C. Different concentrations of Dox or cyclic $[W(RW)_4]$−Dox (up to a maximum of 10 μM) were incubated with the cells for 2 h. Compounds were removed from medium by replacing with fresh medium, and the cells were kept in an incubator for another 72 h. The cells without compounds were included in each experiment as controls. After 72 h of incubation, 20 μL of MTS was added and incubated for 2 h. The absorbance of the formazan product was measured at 490 nm using microplate reader. The percentage of cytotoxicity was calculated as [(OD value of untreated cells) − (OD value of treated cells)]/(OD value of untreated cells) × 100%.

Confocal Microscopy. SK-OV-3 cells were seeded with EMEM media overnight on coverslips in six well plates. Then the medium was removed and washed with opti-MEM. The cells were treated with Dox or cyclic $[W(RW)_4]$−Dox (5 μM) in opti-MEM for 1 h at 37 °C. After 1 h incubation, the media containing the compound were removed followed by washing with PBS three times. Then coverslips were placed on a drop of mounting medium on a microscope slide with cell-attached side facing down. Laser scanning confocal microscopy was carried out using a Carl Zeiss LSM 510 system. The cells were imaged using rhodamine and phase contrast channels. In the case of drug efflux studies, after a 1 h incubation period, the medium containing drugs was removed and washed with opti-MEM. Then fresh medium with serum was added into the cells. After 24 h, the medium was removed and washed with PBS three times, and then the cells were visualized under confocal microscopy.

Fluorescence Activated Cell Sorter (FACS) Analysis of Cellular Uptake Experiment. Ovarian carcinoma cells were plated overnight in six well plates (2×10^5 cells/well) in EMEM media. Then Dox (5 μM), cyclic $[W(RW)_4]$−Dox (5 μM), linear $(RW)_4$−Dox (5 μM), cyclic $[RW]_4$ (5 μM) + Dox (5 μM), and $(RW)_4$ (5 μM) + Dox (5 μM) were added in serum-free RPMI to the cells. For the physical mixtures, an appropriate volume of Dox stock solution was mixed with an appropriate volume of an aqueous solution of cyclic and linear peptides physically to obtain a final concentration of Dox (5 μM) and CPPs (5 μM). The mixture was vigorously mixed and vortexed until the solution became homogeneous/clear red color. Subsequently, the mixture was incubated for 30 min at 37 °C before addition to the cells. The plates were incubated for 1 h at 37 °C. After 1 h incubation, the media containing drugs were removed. The cells were digested with 0.25% trypsin/0.53 mM EDTA for 5 min to detach from the plate. Then the cells were centrifuged and washed twice with PBS. Finally, the cells were resuspended in flow cytometry buffer and analyzed by flow cytometry (FACSCalibur: Becton Dickinson) using FL2 channel and CellQuest software. The data presented are based on the mean fluorescence signal for 10,000 cells collected. All assays were performed in triplicate.

Fluorescence Activated Cell Sorter (FACS) Analysis of Cell Cycle Arrest. Colorectal carcinoma cells (2×10^5 per well) were treated with cyclic $[W(RW)_4]$−Dox at 1 μM for 1 h followed by 24 h incubation in drug-free medium. Cells were fixed in ice-cold ethanol:PBS (70:30, v/v) for 30 min at 4 °C, further resuspended in PBS with 100 μg/mL RNase and 40 μg/mL propidium iodide, and incubated at 37 °C for 30 min. The DNA content (for 10,000 cells) was analyzed using a FACSCalibur instrument equipped with FACStation with FACSCalibur software (BD Biosciences, San Diego, CA, USA). The analyses of cell cycle distribution were performed in triplicate (n = 2 plates per experiment) for the sample treatment. The coefficient of variation, according to the ModFit LT Version 2 acquisition software package (Verity Software House, Topsham, ME, USA), was always less than 5%.

Topo II Decatenation Assay. The topoisomearase II assay kit (Catalog No. 1001-1) was purchased from TopoGEN, Inc. (Port Orange, FL). Eukaryotic Topo II was assayed by decatenation of kDNA and monitoring the appearance of a smaller DNA (decatenated DNA circles). Reaction mixtures containing kDNA (0.1 μg) in a final volume of 20 μL and 1× reaction buffer containing Tris-HCl (50 mM, pH 8.0), NaCl (150 mM), $MgCl_2$ (10 mM), dithiothreitol (0.5 mM), and ATP (2 mM) were incubated for 30 min at 37 °C without and with Dox, and cyclic $[W(RW)_4]$−Dox at 10, 20, 30, 40, and 50 μM final concentration. Reactions were terminated with the addition of 0.4 volume of stop buffer (5% sarkosyl, 0.125% bromophenol blue, and 25% glycerol). One unit of Topo II is defined as the amount of enzyme required to fully decatenate 0.1 μg of kDNA in 30 min at 37 °C. The decatenation products were analyzed on 1% agarose gels having 0.5 μg of ethidium bromide/mL. Eukaryotic Topo II products were separated at 108 V, which allowed rapid resolution of catenated networks from the minicircles. Gels were photographed by ethidium bromide fluorescence on Typhoon Imager.

Stability Studies. The stability of cyclic $[W(RW)_4]$−Dox was evaluated using phosphate-buffered saline (PBS) and fetal bovine serum (FBS). PBS and FBS were purchased from Invitrogen and ATCC (Manassas, VA). FBS (1 mL, 100%) and PBS (1 mL, pH 7.0) were incubated with cyclic $[W(RW)_4]$−Dox (75 μL, 1 mM in water) at 37 °C followed by intermediate mixing. An aliquot of 75 μL of the mixture was taken out at different time intervals (10 min to 96 h) and diluted with water (75 μL). The mixture was analyzed by using analytical HPLC detecting the wavelength of 490 nm. The area under the curve (AUC) was calculated and used to find out the percentage of released Dox and remaining prodrug at a given time. Figure S5 (Supporting Information) was plotted between relative percentage of released Dox and cyclic $[W(RW)_4]$−Dox based on HPLC analysis.

Cellular Hydrolysis. Intracellular hydrolysis of cyclic $[W(RW)_4]$−Dox and accumulation of Dox and the peptide−Dox conjugate were determined in CCRF-CEM cells by HPLC analysis. CCRF-CEM cells were grown in 75 cm^2 culture flasks with serum-free RPMI medium to ∼70−80% confluence (1.37×10^7 cells/mL). The medium was replaced with fresh RPMI medium having cyclic $[W(RW)_4]$−Dox (1 μM), and the cells were incubated at 37 °C for 4 h. The medium containing cyclic $[W(RW)_4]$−Dox was carefully removed by using centrifugation

and replaced with fresh RPMI serum-free medium. The cells were partitioned/transferred to culture plates (six well) having 1.37×10^7 cells per well in 5 mL of medium and incubated for the indicated time. After incubation, the cells were collected by centrifugation. The medium was removed carefully by decantation, and cell pellets were washed with ice-cold PBS to remove any medium. The cell pellets were thoroughly extracted with an equal volume of methanol, chloroform, and isopropanol mixture (4:3:1 v/v/v) and filtered through 0.2 μm filters. The relative Dox and cyclic $[W(RW)_4]$−Dox concentrations in cell lysates were quantified by analytical HPLC analysis as described in the Supporting Information at 490 nm using the water/acetonitrile solvent method.

RESULTS AND DISCUSSION

Chemistry. Linear and cyclic peptides were synthesized by Fmoc/*t*Bu solid-phase peptide synthesis. Scheme 1 depicts the synthesis of linear peptide $(RW)_4$ on the Rink amide resin. The linear peptide sequence was assembled using a PS3 peptide synthesizer. The last Fmoc group on the *N*-terminal was deprotected by piperidine (20% v/v, DMF). The resin was dried, washed, and cleaved by cleavage cocktail (reagent R) to afford the linear $(RW)_4$, which was purified by reversed-phase Hitachi HPLC.

For the synthesis of the cyclic peptide, first the linear protected peptide (Dde-K(Boc-β-Ala)(WRWRWRWRW) was assembled on the H-Trp(Boc)-2-chlorotrityl chloride resin. The Dde group of *N*-terminal lysine was removed in the presence of hydrazine (2% in DMF). The side chain protected peptide was cleaved from the resin using AcOH/TFE/DCM (1:2:7 v/v/v) cocktail. The cyclization of the side chain protected peptide was performed under pseudodilute conditions in the presence of HOAt and DIC (Scheme 2). The cyclic peptide was cleaved in the presence of reagent R, purified using reversed-phase HPLC, and used for the conjugation with Dox.

N-Fmoc-Dox-14-*O*-hemiglutrate was prepared as described previously.[33] In brief, the reaction of glutaric anhydride with Fmoc-protected Dox was carried out to produce the Dox hemiglutarate ester with a free COOH, which after HPLC purification and lyophilization was used for coupling with linear and cyclic peptides. The conjugation of the peptides with *N*-Fmoc-Dox-14-*O*-hemiglutrate was achieved in a similar pattern (Scheme 3). The equimolar amount of the peptide and Dox was coupled through formation of an amide bond between the amino group of peptides and carboxylic acid in the Fmoc-protected Dox. The carboxylic group in Fmoc-protected Dox was preactivated in the presence of HOAt/PyBOP/DIPEA in DMF for 15 min before reacting with the peptides. After conjugation, the Fmoc protecting group was removed using piperidine and was then acidified. The coupled peptide was purified using HPLC and lyophilized. The structures of all the final compounds were confirmed by a high-resolution MALDI TOF/TOF mass spectrometer. The purity of the final product (≤95%) was confirmed by reversed-phase analytical HPLC using a gradient system with water (0.1% TFA) and acetonitrile as eluting solvents.

Biological Activities. *Cytotoxicity and Antiproliferative Activity of Peptide−Dox Derivatives.* Cyclic $[WR]_4$ and cyclic $[W(RW)_4K](\beta$-Ala) did not show any significant toxicity in MDA-MB-468, HCT-116, CCRF-CEM, and SK-OV-3 cells at a concentration of 10 μM (Figure 1) after different incubation times including 24 h, 72 h, and 120 h. These data are consistent

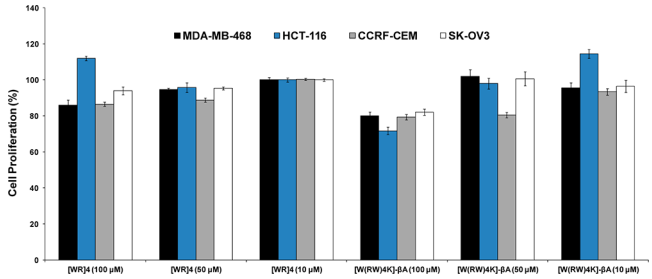

Figure 1. Cytotoxicity assay of cyclic $[WR]_4$ and cyclic $[W(RW)_4K]$-(β-Ala) in MDA-MB-468, HCT-116, CCRF-CEM, and SK-OV-3.

with previously reported data of cyclic $[WR]_4$.[32] Thus, a noncytotoxic concentration of 1 μM was selected for cell-based studies of cyclic peptide conjugate cyclic $[W(RW)_4]$−Dox and the physical mixture cyclic $[RW]_4$ + Dox. We recently compared the toxicity of $[WR]_4$ versus commonly used cell-penetrating peptides and transporters including polyArg CR7, TAT (YGRKKRRQRRRC) (100 μM), and oligofectamine 2000 (Invitrogen, a cationic lipid formulation).[34] $[WR]_4$ did not show any significant toxicity in human ovarian adenocarcinoma (SK-OV-3) and human leukemia (CCRF-CEM) cancer cells and normal human colon myofibroblast (CCD-18Co) cells, while other cell-penetrating peptides polyArg CR7, TAT (YGRKKRRQRRRC), and oligofectamine 2000 (Invitrogen, a cationic lipid formulation) reduced the viability by 21−55%.

The activity of compounds on the cell proliferation of different cancer cells, CCRF-CEM, SK-OV-3, HCT-116, and MDA-MB-468, was investigated for up to 120 h at the concentration of 1 μM. The activity of synthesized compounds, linear $(RW)_4$−Dox and cyclic $[W(RW)_4]$−Dox, was evaluated in a comparative study with the noncovalent physical mixtures of linear $(RW)_4$ + Dox and cyclic $[RW]_4$ + Dox, and Dox alone (Figure 2).

Cyclic $[W(RW)_4]$−Dox exhibited higher antiproliferative activity than linear $(RW)_4$−Dox in all cancer cells, with the highest activity observed after 72 h. The effect of compounds was found to be time dependent. The cell proliferation inhibitory activity of compounds was enhanced at longer incubation period of compounds with cells presumably because of the hydrolysis of the conjugate to Dox. Cyclic $[W(RW)_4]$−Dox inhibited the cell proliferation of CCRF-CEM (62−73%), SK-OV-3 (51−74%), HTC-116 (50−67%), and MDA-MB-468 (60−79%) cells at a concentration of 1 μM after 72−120 h of incubation, while linear $(RW)_4$−Dox exhibited antiproliferative activity against CCRF-CEM (46−69%), SK-OV-3 (28−34%), HTC-116 (21−61%), and MDA-MB-468 (60−74%) under similar conditions. These data suggest that cyclization of peptide provided a more effective transporter for Dox. The antiproliferative activity of cyclic $[W(RW)_4]$−Dox was in the order MDA-MB-468 > CCRF-CEM > SK-OV-3 > HTC-116.

In general, the physical mixture of linear $(RW)_4$ and cyclic $[RW]_4$ with Dox derivative showed less antiproliferative activity in comparison to cyclic $[W(RW)_4]$−Dox conjugate after 72−120 h against CCRF-CEM (52−68%), SK-OV-3 (47−67%), and HTC-116 (38−62%), and showed slightly better or comparable activity against MDA-MB-468 (71−78%). Dox exhibited also similar antiproliferative activity in comparison to the physical mixture against CCRF-CEM (59−71%), SK-OV-3 (48−59%), HTC-116 (37−64%), and MDA-MB-468 (71−77%) after 72−120 h of incubation, indicating that conjugation

dx.doi.org/10.1021/mp3004034 | *Mol. Pharmaceutics* 2013, 10, 488−499

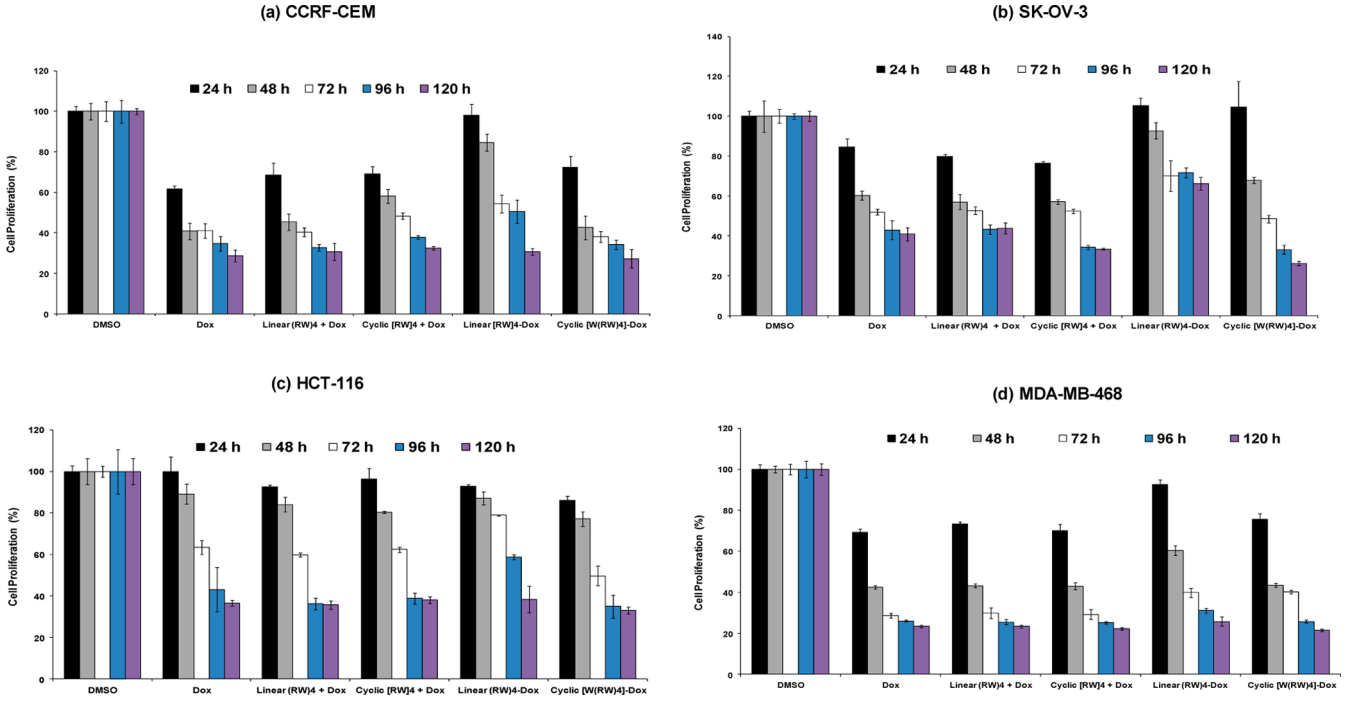

Figure 2. Inhibition of (a) CCRF-CEM, (b) SK-OV-3, (c) HCT-116, and (d) MDA-MB-468 cells by compounds (1 μM) after 24−120 h incubation. The results are shown as the percentage of the control DMSO that has no compound (set at 100%). All the experiments were performed in triplicate (±SD).

of the cyclic peptide with Dox in cyclic $[W(RW)_4]$−Dox improved the antiproliferative activity of Dox in some of the tested cancer cells. The cyclic peptide−Dox conjugate showed comparable antiproliferative activity against CCRF-CEM and MDA-MB-468 when compared to Dox after 96 and 120 h incubation. However, the antiproliferative activities of cyclic $[W(RW)_4]$−Dox conjugate in SK-OV-3 and HCT-116 cells were higher than those of Dox at a concentration of 1 μM after 96 and 120 h incubation. For example, cyclic $[W(RW)_4]$−Dox inhibited the cell proliferation of SK-OV-3 (67−74%) and HTC-116 (65−67%) cells at a concentration of 1 μM after 96−120 h of incubation, while Dox exhibited antiproliferative activity against SK-OV-3 (57−59%) and HTC-116 (57−64%) under similar conditions.

Cyclic [W(RW)$_4$]−Dox Showed Higher Cellular Retention Than Dox and Linear (RW)$_4$−Dox. Dox is easy to track by using fluorescence-based techniques, due to the inherent red fluorescence. Because of the higher antiproliferative activity of cyclic $[W(RW)_4]$−Dox after 72 h compared to linear $(RW)_4$−Dox and Dox, this compound was selected for further cellular uptake studies in comparison to other compounds to determine whether the higher activity of this compound is consistent with enhanced uptake of the compound.

The cellular uptake of all derivatives was examined in Dox-resistant SK-OV-3 cells using fluorescence-activated cell sorter (FACS) analysis (Figure 3). To obtain the primary influx, cells were allowed to be incubated with covalent cyclic $[W(RW)_4]$−Dox and linear $(RW)_4$−Dox peptides, noncovalent physical mixtures, cyclic $[W(RW)_4]$ + Dox and linear $(RW)_4$ + Dox, and Dox for 1 h. This process was followed by 24 h incubation with media to allow the cells to start the efflux process through pumping the compounds out. Then the amounts of Dox in cells were evaluated by using FACS in Dox-resistant SK-OV-3 cells. The data showed 3.3−3.6-fold more cellular uptake of cyclic $[W(RW)_4]$−Dox compared to Dox alone and noncovalent

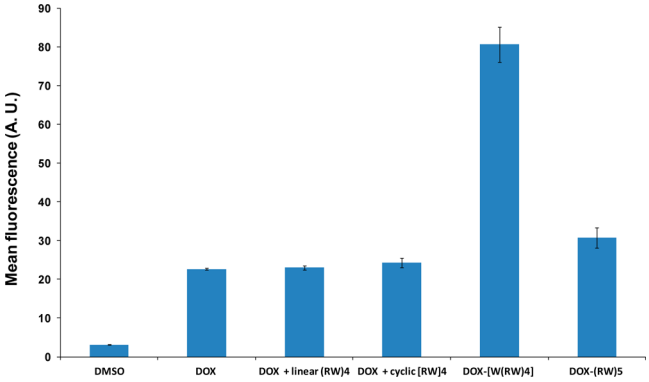

Figure 3. FACS analysis of cellular uptake assays of cyclic $[W(RW)_4]$−Dox (5 μM) in SK-OV-3 cells compared with linear $(RW)_4$−Dox (5 μM) and the physical mixtures, cyclic $[RW)_4]$ (5 μM) + Dox (5 μM) and linear $(RW)_4$ (5 μM) + Dox (5 μM).

physical mixtures, cyclic $[W(RW)_4]$ + Dox and linear $(RW)_4$ + Dox, in SK-OV-3 (Figure 3). Between linear and cyclic peptide−Dox covalent conjugates, the retention of cyclic $[W(RW)_4]$−Dox was found to be 2.6-fold higher compared to that of linear $(RW)_4$−Dox. These data suggest that cyclic peptide−Dox, cyclic $[W(RW)_4]$−Dox, enhanced the cellular uptake of the compound. The cyclic nature of the peptide was found to contribute in inhibition of the efflux. These data are consistent with higher antiproliferative activity of cyclic $[W(RW)_4]$−Dox versus linear $(RW)_4$−Dox and Dox, suggesting that the presence of cyclic peptide in the conjugate reduces efflux, increases cellular uptake and retention of Dox, and enhances antiproliferative activity.

Cyclic [W(RW)$_4$]−Dox Nuclear Localization in SK-OV-3 Cells. The cellular localization of free Dox and conjugate cyclic $[W(RW)_4]$−Dox was compared in SK-OV-3 cells after 1 and

dx.doi.org/10.1021/mp3004034 | *Mol. Pharmaceutics* 2013, 10, 488−499

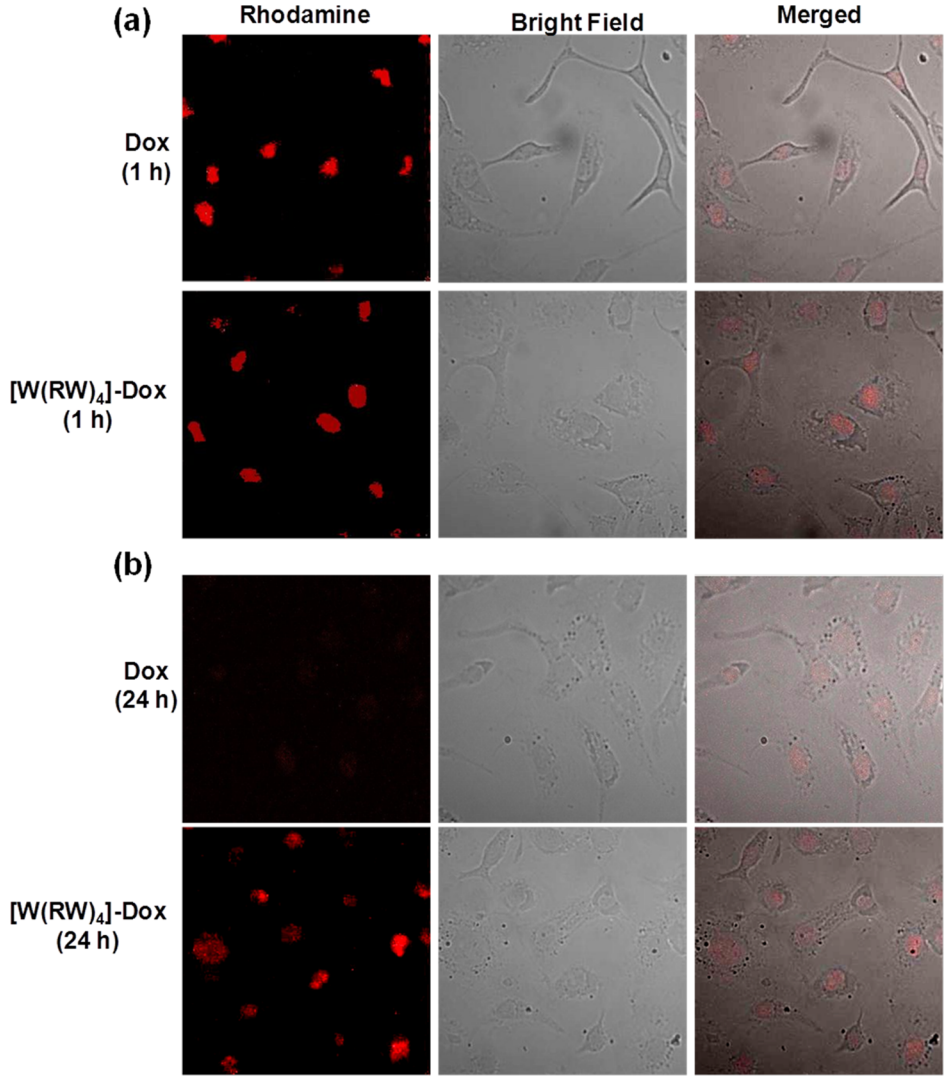

Figure 4. (a) Confocal microscopy images of Dox and cyclic $[W(RW)_4]$−Dox (5 μM) uptake in SK-OV-03 cells after 1 h. Red represents the fluorescence of Dox. (b) Confocal microscopy images of Dox and cyclic $[W(RW)_4]$−Dox (5 μM) uptake in SK-OV-03 cells. SK-OV-3 cells were treated with the compound for 1 h. The compound was removed, and the cells were incubated with complete media for 24 h. Red represents the fluorescence of Dox.

24 h incubation at 37 °C. A noncytotoxic concentration of 5 μM was chosen to ensure Dox fluorescence detection by confocal microscopy. Confocal microscopy images of SK-OV-3 cells are shown after 1 h incubation. Free Dox and cyclic $[W(RW)_4]$−Dox were localized mainly in the nucleus (Figure 4a). The results showed that the covalent conjugation of Dox with cyclic $[W(RW)_4]$ did not prevent the nuclear accumulation of the drug. To compare the retention ability of cyclic $[W(RW)_4]$−Dox versus Dox alone against efflux effects, SK-OV-3 cells were incubated with both compounds for 1 h followed by incubation in drug-free media for 24 h at 37 °C. The fluorescence intensity of Dox in cells treated with cyclic $[W(RW)_4]$−Dox was found to be significantly higher than that in cells treated with Dox alone (Figure 4b), indicating that cyclic $[W(RW)_4]$−Dox was retained in cells much longer than free Dox. Thus, this conjugate has a potential to be used as a tool for enhancing the nuclear retention of Dox.

Stability of Cyclic [W(RW)$_4$]−Dox. Cyclic $[W(RW)_4]$−Dox was incubated with phosphate-buffered saline (PBS) and fetal bovine serum (FBS) solution at 37 °C at different time intervals. The results indicated that cyclic $[W(RW)_4]$−Dox is relatively stable in both systems with half-life values of 10.77 and 26.20 h in PBS and FBS, respectively. No interaction between serum proteins and cyclic $[W(RW)_4]$−Dox was observed since the mixture was clear and no precipitation or turbidity was found during the assay. Cyclic $[W(RW)_4]$−Dox was found to be stable in PBS (97%) and FBS (84%) after 1 h. For cellular uptake studies using FACS, the cells were incubated by cyclic $[W(RW)_4]$−Dox for 1 h followed by 24 h incubation with drug-free media. During the 1 h period, the compound showed minimal hydrolysis in serum, suggesting that most of the compound is hydrolyzed intracellularly (Figures S5 and S6 in the Supporting Information).

Intracellular Hydrolysis. Intracellular hydrolysis results for cyclic $[W(RW)_4]$−Dox were monitored in CCRF-CEM cells. CCRF-CEM cells (1.37×10^7) were incubated with the conjugate (1 μM) for 4 h followed by drug-free medium to determine the possibility of the intracellular hydrolysis to Dox. Drug-free medium was used to rule out the continuous cellular uptake of the conjugate, while the compound is hydrolyzed intracellularly. HPLC analysis with detection at 490 nm and at specific time intervals after cellular lysis was used to measure

dx.doi.org/10.1021/mp3004034 | *Mol. Pharmaceutics* 2013, 10, 488−499

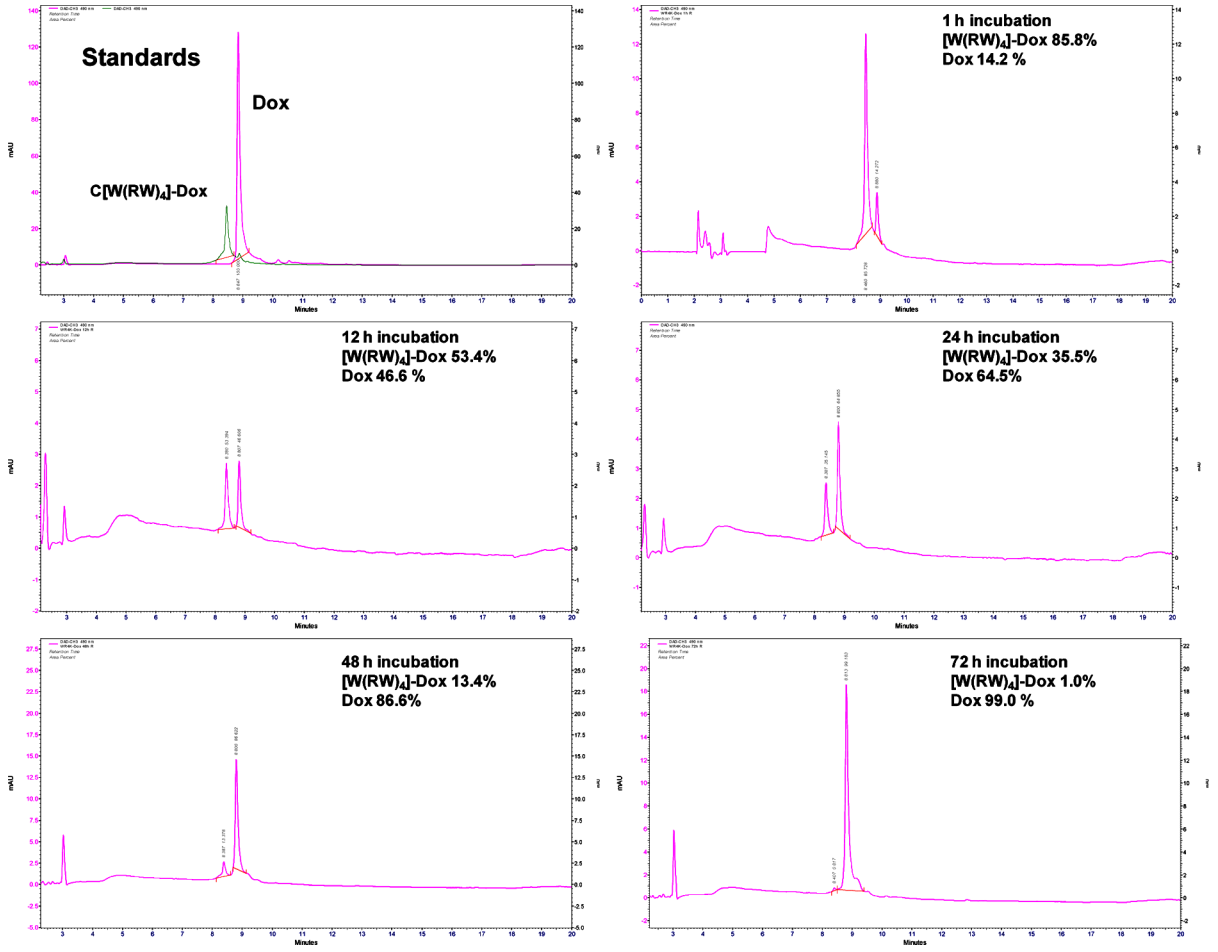

Figure 5. HPLC chromatograms for the cellular uptake studies of cyclic [W(RW)$_4$]−Dox using CCRF-CEM cells after incubation for 1−72 h.

the ratio of the cyclic [W(RW)$_4$]−Dox and released Dox. The cellular hydrolysis data exhibited that the cyclic peptide−Dox conjugate was hydrolyzed intracellularly and released Dox in a time-dependent manner. More than 46% of cyclic [W(RW)$_4$]−Dox was hydrolyzed intracellularly within 12 h. Approximately 86% of cyclic [W(RW)$_4$]−Dox was hydrolyzed intracellularly within 48 h (Figure 5). These data suggest that the enhanced uptake, retention, and sustained intracellular hydrolysis of cyclic [W(RW)$_4$]−Dox to Dox contribute to overall activity of the conjugate as a potential prodrug.

Cell Cycle Distribution Analysis. In addition to apoptosis,[35,36] Dox treatment causes cell cycle arrest in cancer cells.[37] The impact of cyclic [W(RW)$_4$]−Dox on cell cycle distribution was investigated in colorectal carcinoma cells (HCT-116) compared to Dox. All experiments were performed under similar conditions, and appropriate controls were used to confirm the results. An hour incubation was selected followed by 24 h incubation in drug-free medium, due to the significant difference in the cellular uptake of cyclic [W(RW)$_4$]−Dox and Dox. Control cells were found in G_0/G_1 phase (46.8 ± 1.0%), S phase (36.5 ± 0.7%), and G_2/M phase (16.5 ± 0.2%). The percentage of the pre-G0/G1 population indicates the apoptosis rate of cells. There was no significant pre-G0-G1 population as shown in the histograms because the cells were incubated with Dox and the prodrug only for 1 h. Cells treated with compounds (Dox and cyclic [W(RW)$_4$]−Dox) showed different patterns than control cells for G_0/G_1 phase (53.0 ± 1.0% and 42.2 ± 1.4%), S phase (21.8 ± 3.0% and 23.5 ± 0.2%), and G_2/M phase (25.1 ± 2.0% and 34.1 ± 1.2%), respectively (Figure 6). The data showed that, in cells treated

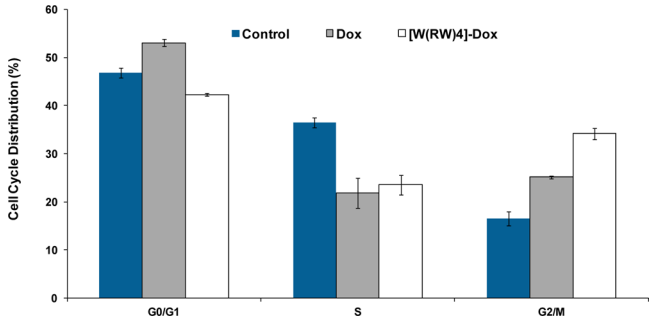

Figure 6. Comparison of cell cycle arrest by Dox and cyclic [W(RW)$_4$]−Dox.

with cyclic [W(RW)$_4$]−Dox, the proportion of cells in G_0/G_1 phase was decreased nearly 10% compared to values for Dox. On the other hand, the proportion of cells in G_2/M phase increased nearly 10% compared to values for Dox. These data suggest that cyclic [W(RW)$_4$]−Dox led to a significant reduction of cells in G_0/G_1 phase, and caused more accumulation in G_2/M phase in HCT-116 cells. This pattern is slightly different when compared to Dox. This could be due to the requirement for cyclic [W(RW)$_4$]−Dox to get hydrolyzed to Dox. Based on the population of cells at different phases, prodrug follows a different pattern when

dx.doi.org/10.1021/mp3004034 | *Mol. Pharmaceutics* 2013, 10, 488−499

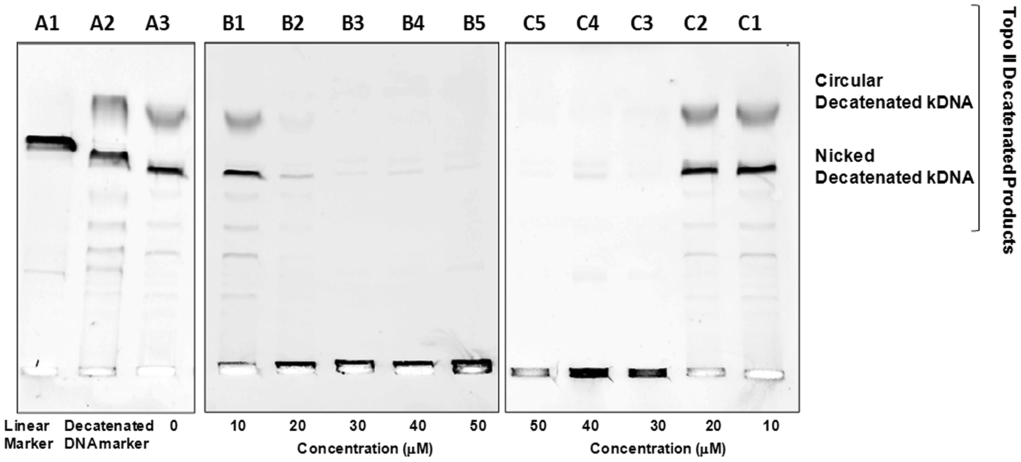

Figure 7. Topo II assay for Dox (middle) and cyclic $[W(RW)_4]$−Dox (right). The lines A1 and A2 were linear markers and decatenated DNA markers, respectively. Line A3 represents the blank kDNA in the absence of any compound. kDNA was incubated with compound Dox (10−50 μM, lanes B1−B5) and cyclic $[W(RW)_4]$−Dox (10−50 μM, lanes C1−C5) and decatenated using topoisomerase II for 30 min at 37 °C. The decatenation was monitored by gel electrophoresis and imaged by ethidium bromide fluorescence.

compared with Dox. Some of the antiproliferative activity by cyclic $[W(RW)_4]$−Dox could be due to the differential pattern of cell cycle distribution by the conjugate, in addition to intracellular hydrolysis to Dox. The histograms were also provided in the Supporting Information (Figure S4).

Topo II Inhibitory Activity. One of the major anticancer mechanisms of Dox is the inhibition of topoisomerase II.[2] Thus, a comparative study was performed between cyclic $[W(RW)_4]$−Dox and Dox to determine whether the conjugate has Topo II inhibitory activity similar to that of the parent drug. Topo II is responsible for catalyzing the DNA double-stranded cleavage process by isolating catenated DNA duplexes. Kinetoplast DNA (kDNA) is used as a DNA substrate in the *in vitro* decatenation assay. The potency of Dox and cyclic $[W(RW)_4]$−Dox to inhibit Topo II enzyme for the decatenation of kDNA was used to analyze the comparative inhibitory activity of the compounds. Topo II decatenation assay exhibited that Dox inhibited Topo II at concentrations between 10 and 20 μM; however cyclic $[W(RW)_4]$−Dox inhibited the Topo II activity at concentrations between 20 and 30 μM (Figure 7) under similar reaction conditions. As expected, the conjugate acts at higher concentration compared to Dox since the conjugate is required to get hydrolyzed to Dox to be able to inhibit Topo II more efficiently. Under the *in vitro* conditions used here, the conjugate is not hydrolyzed and the reduced Topo II inhibitory activity is possibly due to the conjugation to the peptide and associated steric hindrance. Hydrolysis to Dox is required to generate maximum Topo II inhibitory activity associated with Dox. The conjugate does not undergo hydrolysis under *in vitro* conditions in this assay.

CONCLUSIONS

In summary, linear and cyclic peptide−Dox conjugates were synthesized as prodrugs, were evaluated for their activities against various cancer cell lines, and were compared with the corresponding physical mixtures. The conjugation of Dox with a specific cyclic peptide, cyclic $[W(RW)_4]$−Dox, improved the antiproliferative activity compared to the corresponding physical mixtures in all tested cell lines. Cyclic peptide−Dox conjugate showed comparable antiproliferative activity against CCRF-CEM and MDA-MB-468 when compared to Dox. However, the antiproliferative activities of cyclic $[W(RW)_4]$−Dox conjugate in SK-OV-3 and HCT-116 cells were higher than those of Dox and linear $(RW)_4$−Dox at a concentration of 1 μM after 96 and 120 h incubation. Dox has short retention time in some cancer cells (e.g., ovarian adenocarcinoma SK-OV-3) due to the efficient efflux effect. Thus, the differential cytotoxicity of cyclic $[W(RW)_4]$−Dox with Dox in SK-OV-3 could be due to the retention of Dox in the presence of the cyclic peptide. Since the system was designed as a prodrug, we did not expect to detect a huge difference between Dox and cyclic $[W(RW)_4]$−Dox in cytotoxicity. Furthermore, we demonstrated that the prodrug approach for Dox using a cyclic peptide conjugate significantly improved the cellular uptake and retention time of Dox in SK-OV-3 cancer cells. Flow cytometry analysis showed 3.3−3.6-fold higher cellular uptake of cyclic $[W(RW)_4]$−Dox than Dox alone and the physical mixtures, cyclic $[W(RW)_4]$ + Dox and linear $(RW)_4$ + Dox, in SK-OV-3 cells after 24 h incubation. The conjugate exhibited nuclear localization and retention after 24 h, and underwent intracellular hydrolysis to Dox in CCRF-CEM cells, suggesting to be a potential prodrug for delivery of the drug. The cellular hydrolysis study showed that 99% of cyclic $[W(RW)_4]$−Dox was hydrolyzed intracellularly within 72 h and released Dox. These data suggest that cyclic $[W(RW)_4]$−Dox can be used as a potential prodrug for improving the biological profile, cellular delivery, and retention of Dox.

ASSOCIATED CONTENT

Supporting Information

Materials and methods, general chemistry, mass spectra, and additional supporting data and figures for stability and cell cycle arrest. This material is available free of charge via the Internet at http://pubs.acs.org.

AUTHOR INFORMATION

Corresponding Author

*7 Greenhouse Road, Department of Biomedical and Pharmaceutical Sciences, College of Pharmacy, University of Rhode Island, Kingston, Rhode Island 02881, United States. Tel: +1-401-874-4471. Fax: +1-401-874-5787. E-mail: kparang@uri.edu.

Notes

The authors declare no competing financial interest.

■ ACKNOWLEDGMENTS

We acknowledge the American Cancer Society, Grant No. RSG-07-290-01-CDD, and the US National Science Foundation, Grant No. CHE 0748555, for the financial support. We thank National Center for Research Resources, NIH, and Grant No. 1 P20 RR16457 for sponsoring the core facility.

■ ABBREVIATIONS USED

CCRF-CEM, human leukemia carcinoma cell line; CPPs, cell-penetrating peptides; DCM, dichloromethane; Dox, doxorubicin; DIPEA, *N*,*N*-diisopropylethylamine; HBTU, DDS, drug delivery systems; FACS, fluorescence activated cell sorter; FBS, fetal bovine serum; DCM, dichloromethane; HCT-116, human colorectal carcinoma; HOBt, hydroxybenzotriazole; HBTU, 1,1,3,3-tetramethyluronium hexafluorophosphate; MDA-MB-468, human breast adenocarcinoma; MRPs, multidrug resistance proteins; NMM, (*N*-methylmorpholine); P-gp, P-glycoprotein; PBS, phosphate buffered saline solution; PyBOP, benzotriazol-1-yloxytripyrrolidinophosphonium hexafluorophosphate; SK-OV-3, human ovarian adenocarcinoma, 1,1,3,3-tetramethyluronium hexafluorophosphate; TOPO II, topoisomerase II

■ REFERENCES

(1) Vincenzi, B.; Frezza, A. M.; Santini, D.; Tonini, G. New therapies in soft tissue sarcoma. *Expert Opin. Emerging Drugs* **2010**, *15*, 237−248.

(2) (a) Quigley, G. J.; Wang, A. H.; Ughetto, G.; van der Marel, G.; van Boom, J. H.; Rich, A. Molecular structure of an anticancer drug-DNA complex: daunomycin plus d(CpGpTpApCpG). *Proc. Natl. Acad. Sci. U.S.A.* **1980**, *77*, 7204−7208. (b) Patel, D. J.; Kozlowski, S. A.; Rice, J. A. Hydrogen bonding, overlap geometry, and sequence specificity in anthracycline antitumor antibiotic.DNA complexes in solution. *Proc. Natl. Acad. Sci. U.S.A* **1981**, *78*, 3333−3337.

(3) Gottesman, M. M. Mechanisms of drug resistance. *Annu. Rev. Med.* **2002**, *53*, 615−627.

(4) Longely, D. B.; Johnston, P. G. Molecular mechanisms of drug resistance. *J. Pathol.* **2005**, *205*, 275−292.

(5) Stavrovskaya, A. A. Cellular mechanisms of multidrug resistance of tumor cells. *Biochemistry* **2000**, *65*, 95−106.

(6) Kratz, F. DOXO-EMCH (INNO-206): The first albumin binding prodrug of doxorubicin to enter clinical trials. *Expert Opin. Invest. Drugs* **2007**, *16*, 855−866.

(7) Tang, Y.; McGoron, A. J. Combined effects of laser-ICG photothermotherapy and doxorubicin chemotherapy on ovarian cancer cells. *J. Photochem. Photobiol., B* **2009**, *97*, 138−144.

(8) Raoul, J. L.; Heresbach, D.; Bretagne, J. F.; Ferrer, D. B.; Duvauferrier, R.; Bourguet, P.; Messner, M.; Gosselin, M. Chemoembolization of hepatocellular carcinomas a study of the biodistribution and pharmacokinetics of doxorubicin. *Cancer* **1992**, *70*, 585−590.

(9) Rahman, A.; Carmichael, D.; Harris, M.; Roh, J. K. Comparative pharmacokinetics of free doxorubicin and doxorubicin entrapped in cardiolipin liposomes. *Cancer. Res.* **1986**, *46*, 2295−2299.

(10) (a) Chhikara, B. S.; St. Jean, N.; Mandal, D.; Kumar, A.; Parang, K. Fatty acyl amide derivatives of doxorubicin: Synthesis and in vitro anticancer activities. *Eur. J. Med. Chem.* **2011**, *46*, 2037−2042. (b) Chhikara, B.S.; Mandal, D.; Parang, K. Synthesis, anticancer activities, and cellular uptake studies of lipophilic derivatives of doxorubicin succinate. *J. Med. Chem.* **2012**, *55*, 1500−1510.

(11) Takemura, G.; Fujiwara, H. Doxorubicin-induced cardiomyopathy from the cardiotoxic mechanisms to management. *Prog. Cardiovasc. Dis.* **2007**, *49*, 330−352.

(12) Ayla, S.; Seckin, I.; Tanriverdi, G.; Cengiz, M.; Eser, M.; Soner, B. C.; Oktem, G. Doxorubicin induced nephrotoxicity: protective effect of nicotinamide. *Int. J. Cell Biol.* **2011**, 390238.

(13) Seelig, A.; Gatlik-Landwojtowicz, E. Inhibitors of multidrug efflux transporters: their membrane and protein interactions. *Mini-Rev. Med. Chem.* **2005**, *5*, 135−151.

(14) Yang, X.; Deng, W.; Fu, L.; Blanco, E.; Gao, J.; Quan, D.; Shuai, X. Folate functionalized polymeric micelles for tumor targeted delivery of a potent multidrug-resistance modulator FG020326. *J. Biomed. Mater. Res., Part A* **2008**, *86*, 48−60.

(15) Chavanpatil, M. D.; Khdair, A.; Gerard, B.; Bachmeier, C.; Miller, D. W.; Shekhar, M. P. V.; Panvam, J. Surfactant-polymer nanoparticles overcome P-glycoprotein-mediated drug efflux. *Mol. Pharmaceutics* **2007**, *4*, 730−738.

(16) Sadava, D.; Coleman, A.; Kane, S. E. Liposomal daunorubicin overcomes drug resistance in human breast, ovarian and lung carcinoma cells. *J. Liposome Res.* **2002**, *12*, 301−309.

(17) Ibsen, S.; Zahavy, E.; Wrasdilo, W.; Berns, M.; Chan, M.; Esener, S. A novel doxorubicin prodrug with controllable photolysis activation for cancer chemotherapy. *Pharm. Res.* **2010**, *27*, 1848−1860.

(18) Chhikara, B. S.; Parang, K. Development of cytarabine prodrugs and delivery systems for leukemia treatment. *Expert Opin. Drug Delivery* **2010**, *7*, 1399−1414.

(19) Wang, Y.; Li, L.; Jiang, W.; Yang, Z.; Zhang, Z. Synthesis and preliminary antitumor activity evaluation of a DHA and doxorubicin conjugate. *Bioorg. Med. Chem. Lett.* **2006**, *16*, 2974−2977.

(20) Kumar, S. A.; Peter, Y. A.; Nadeau, J. L. Facile biosynthesis, separation and conjugation of gold nanoparticles to doxorubicin. *Nanotechnology* **2008**, *19*, 495101.

(21) You, J.; Zhang, G.; Li, C. Exceptionally high payload of doxorubicin in hollow gold nanosphere for near-infrared light triggered drug release. *ACS Nano* **2010**, *4*, 1033−1041.

(22) Massing, U.; Fuxius, S. Liposomal formulations of anticancer agents: selectivity and effectiveness. *Drug Resist. Updates* **2000**, *3*, 171−177.

(23) Derossi, D.; Joliot, A. H.; Chassaing, G.; Prochiantz, A. The third helix of the Antennapedia homeodomain translocates through biological membranes. *J. Biol. Chem.* **1994**, *269*, 10444−10450.

(24) Derossi, D.; Chassaing, G.; Prochiantz, A. Trojan peptides: the penetratin system for intracellular delivery. *Trends Cell Biol.* **1998**, *8*, 84−87.

(25) Meyer-Losic, F.; Quinonero, J.; Dubois, V.; Alluis, B.; Dechambre, M.; Michel, M.; Cailler, F.; Fernandez, A. M.; Trouet, A.; Kearsey, J. Improved therapeutic efficacy of doxorubicin through conjugation with a novel peptide drug delivery technology (Vectocell). *J. Med. Chem.* **2006**, *49*, 6908−6916.

(26) Ché, C.; Yang, G.; Thiot, C.; Lacoste, M.-C.; Currie, J.-C.; Demeule, M.; Régina, A.; Béliveau, R.; Castaigne, J.-P. New angiopep modified doxorubicin (ANG1007) and etoposide (ANG1009) chemotherapeutics with increased brain penetration. *J. Med. Chem.* **2010**, *53*, 2814−2824.

(27) Lindgren, M.; Rosenthal-Aizman, K.; Saar, K.; Eiriksdottir, E.; Jiang, Y.; Sassian, M.; Ostlund, P.; Hallbrink, M.; Langel, U. Overcoming methotrexate resistance in breast cancer tumour cells by the use of a new cell-penetrating peptide. *Biochem. Pharmacol.* **2006**, *71*, 416−425.

(28) Zhu, S.; Hong, M.; Zhang, L.; Tang, G.; Jiang, Y.; Pei, Y. PEGylated PAMAM dendrimer-doxorubicin conjugates: In vitro evaluation and in vivo tumor accumulation. *Pharm. Res.* **2010**, *27*, 161−174.

(29) Lee, J.-Y.; Choi, Y.-S.; Suh, J.-S.; Kwon, Y.-M.; Yang, V. C.; Lee, S.-J.; Chung, C.-P.; Park, Y.-J. Cell-penetrating chitosan/doxorubicin/TAT conjugates for efficient cancer therapy. *Int. J. Cancer* **2011**, *128*, 2470−2480.

(30) Shi, N.-Q.; Gao, W.; Xiang, B.; Qi, X.-R. Enhancing cellular uptake of activable cell-penetrating peptide−doxorubicin conjugate by enzymatic cleavage. *Int. J. Nanomed.* **2012**, *7*, 1613−1621.

(31) Aroui, S.; Ram, N.; Appaix, F.; Ronjat, M.; Kenani, A.; Pirollet, F.; De, Waard, M. Maurocalcine as a non toxic drug carrier overcomes doxorubicin resistance in the cancer cell line MDA-MB 231. *Pharm. Res.* **2009**, *28*, 836−845.

(32) Mandal, D.; Nasrolahi Shirazi, A.; Parang, K. Cell-penetrating homochiral cyclic peptides as nuclear-targeting molecular transporters. *Angew. Chem., Int. Ed.* **2011**, *50*, 9633−9637.
(33) Nagy, A.; Schally, A. V.; Armatis, P.; Szepeshazi, K.; Halmos, G.; Miyazaki, M.; Jungwirth, A.; Horvath, J. Cytotoxic analogs of luteinizing hormone-releasing hormone containing doxorubicin or 2-pyrrolinodoxorubicin, a derivative 500−1000 times more potent. *Proc. Nat. Acad. Sci. U.S.A.* **1996**, *93*, 7269−7273.
(34) Nasrolahi Shirazi, A.; Mandal, D.; Tiwari, R. K.; Guo, L.; Lu, W.; Parang, K. Cyclic peptide-capped gold nanoparticles as drug delivery systems. *Mol. Pharmaceutics* **2012**, DOI: 10.1021/mp300448k.
(35) Swift, L. P.; Rephaeli, A.; Nudelman, A.; Philips, D. R.; Cutts, S. M. Doxorubicin-DNA adducts induce a non-topoisomerase II-mediated form of cell death. *Cancer* **2006**, *66*, 4893−4871.
(36) Tsang, W. P.; Chau, S. P. Y.; Kong, S. K.; Fung, K. P.; Kwok, T. T. Reactive oxygen species mediate doxorubicin induced p53-independent apoptosis. *Life Sci.* **2003**, *73*, 2047−2058.
(37) Kim, H. S.; Lee, Y. S.; Kim, D. K. Doxorubicin exerts cytotoxic effects through cell cycle arrest and fas-mediated cell death. *Pharmacology* **2009**, *84*, 300−309.